Exploring ULXs as Short GRB Precursors

L. Nyadzani[1], S. Razzaque[1], and J.D. Finke[2]

University of Johannesburg, Department of Physics[1]

U.S. Naval Research Laboratory[2]

11 July 2025

Centre for Astro-Particle Physics

Outline

- Stellar evolution
- Research Objectives
- Method and ULX model
- Results
- Summary

DCO formation channels:

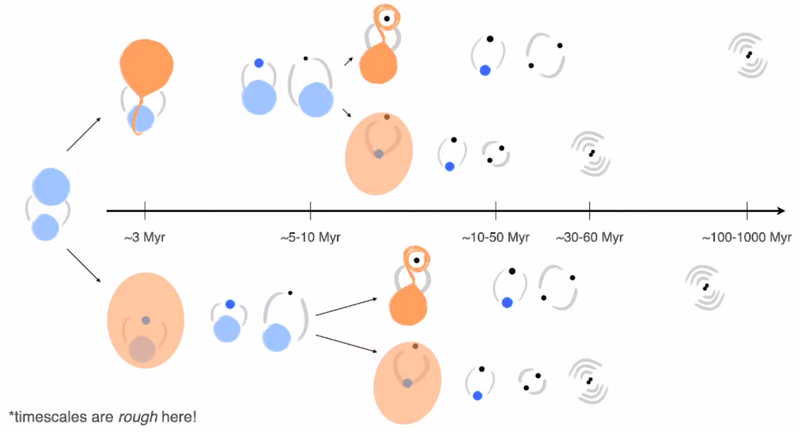

What are ULXs

Ultra-Luminous X-ray sources (ULXs) are galactic point-like sources, exhibiting high X-ray luminosity ($L_x > 10^{39}$ erg/s) exceeding the Eddington limit of neutron stars or stellar-mass black holes (Fabbiano 1989).

- Early surveys identified 16 ULXs with $L_x > 10^{39}$ erg/s (Fabbiano 1989).
- Over 1800 ULXs identified so far (Walton et al. 2022).
- ULXs mainly in extragalactic regions, not in nuclei, are distinct from accreting supermassive black holes.

Research Objectives

- Simulate binary systems (using a population synthetic code)
- Predict DCO merger rates from ULX phase evolution.
- Predict SGRB rates from DNS that evolved through the ULX phase.

Methodology: COSMIC

- **COSMIC (Compact Object Synthesis and Monte Carlo Investigation Code) developed by Breivik et al. (2020):**
  - Population synthesis code used for simulating the evolution of binary systems.
  - Combines theoretical models of stellar evolution, binary interactions, and compact object mergers.
- **Initial Set-up:**
  - Primary star mass (M_1) drawn from a Kroupa initial mass function (IMF) (Kroupa et al. 1993).
  - Secondary star mass (M_2) drawn from a flat distribution of the binary mass ratio ($q = M_2/M_1$).
- **Simulation Details:**
  - Simulated 2×10^6 binary systems at different metallicities (0.5% to 150% $Z_\odot$).
  - Evolved binaries from ZAMS to X-ray binary phase and then to the formation of DCO.
  - Allowed super-Eddington accretion up to 1000 times Eddington rate.

Disc Model

We adopt the SCAD model (Vinokurov et al. 2013).

$$T(r) = T_{\rm in} \begin{cases} (r \sin\theta_f)^{-1/2}, & 1 \le r \le r_{\rm sp} \\ \left[\frac{f_{\rm out}}{\sin\theta_f}(1 + \ln \dot{m})\right]^{1/4} r^{-1/2}, & r_{\rm sp} \le r \le r_{\rm ph} \end{cases}$$

- $T_{\rm in}^4 = \frac{L_{\rm Edd}\sin(\theta_f)}{4\pi\sigma R_{\rm in}^2}$, $R_{\rm in} = 3R_{\rm Sch}$ and σ is the Stefan-Boltzmann constant.
- $\theta_f = 45^\circ$ is the funnel angle.
- $f_{\rm out} = 0.03$ is the fraction of bolometric flux thermalised in the disc.
- $\dot{m} = \dot{M}/\dot{M}_{\rm Edd}$.

$$L_\nu = 2\pi R_{\rm in}^2 \int_1^{r_{\rm ph}} B_\nu(T(r))\, r\, dr\ .$$

ULX population: $L_{\rm X} > 1.26 M_{\rm c} \times 10^{38}$ erg/s using 0.2-12 keV band.

Results: ULX Phase

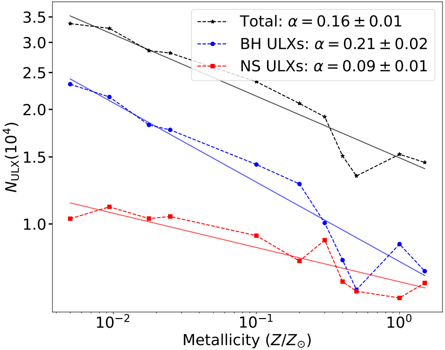

Metal-poor massive stars are more likely to undergo direct collapse into BHs.

The power-law index α varies with metallicity: Low-metallicity environments produce more high-luminosity ULXs.

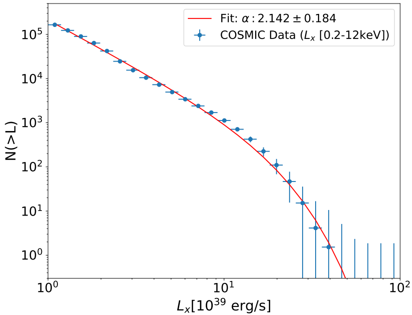

Results: More on ULX Properties

A&A, 695, A8 (2025)
https://doi.org/10.1051/0004-6361/202449208

Astronomy & Astrophysics

A synthetic population of ultra-luminous X-ray sources

Optical–X-ray correlation

Lutendo Nyadzani[1,⋆], Soebur Razzaque[1,2,3,⋆], and Justin D. Finke[4,⋆]

[1] Centre for Astro-Particle Physics (CAPP) and Department of Physics, University of Johannesburg, PO Box 524, Auckland Park 2006, South Africa
[2] Department of Physics, The George Washington University, Washington, DC 20052, USA
[3] National Institute for Theoretical and Computational Sciences (NITheCS), Private Bag X1, Matieland, South Africa
[4] U.S. Naval Research Laboratory, Code 7653, 4555 Overlook Ave. SW, Washington, DC 20375-5352, USA

Received 11 January 2024 / Accepted 21 January 2025

ABSTRACT

This paper presents an analysis of the predicted optical-to-X-ray spectral index (α_{ox}) within the context of ultra-luminous X-ray sources (ULXs) associated with stellar-mass black holes (BHs) and neutron stars (NSs). We used the population synthesis code COSMIC to simulate the evolution of binary systems and investigate the relationship between ultraviolet (UV) and X-ray emission during the ULX phase, namely the α_{ox} relation. Furthermore, we investigated the impact of metallicity on α_{ox} values. Notably, it predicts a significant anti-correlation between α_{ox} and UV luminosity (L_{UV}), consistent with observations. The slope of this relationship varies with metallicity for black hole ULXs (BH-ULXs). The neutron star ULX (NS-ULX) population shows a relatively consistent slope around −0.33 across metallicities, with minor variations. The number of ULXs decreases with increasing metallicity, consistent with observational data. The X-ray luminosity function (XLF) shows a slight variation in its slope with metallicity, exhibiting a relative excess of high-luminosity ULXs at lower metallicities. The inclusion of the beaming effect in the analysis shows a significant impact on the XLF and α_{ox}, particularly at high accretion rates, where the emission is focused into narrower cones. We found that UV emission in ULXs is predominantly disc-dominated, which is the likely origin of the α_{ox} relation, with the percentage of disc-dominated ULXs increasing as metallicity rises.

Key words. binaries: general

Results: Post-ULX Compact Binary Properties

Higher metallicity increases stellar wind mass loss, reducing the number of massive stars and leading to lower DCO formation rates.

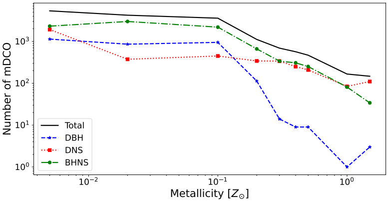

Less than 10% of ULXs evolve to mDCOs, but a striking 70 – 97% of mDCOs trace their evolutionary history through a ULX phase.

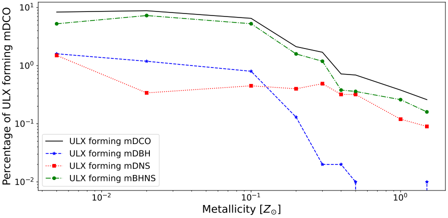

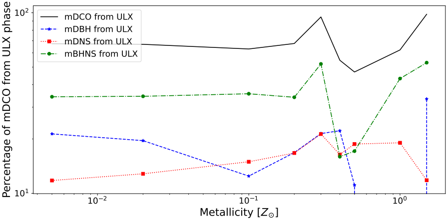

Results: GRB rate Predictions

$$\mathcal{R}_{\rm SGRB} = \int f_{\rm b}(\theta_{\rm jet})\, P(\theta_{\rm jet})\, d\theta_{\rm jet} \times \left(f_{\rm jet,DNS}\, \mathcal{R}_{\rm DNS} + f_{\rm jet,BHNS}\, \mathcal{R}_{\rm BHNS} \right)$$

- $P(\theta_{\rm jet})$ is the log-normal probability density function.
- $f_{\rm jet,DNS} = \frac{N_{\rm DNS->BH}}{N_{\rm DNS,total}}$
- $f_{\rm jet,BHNS} = \frac{N_{\rm BHNS}:(q>0.2)}{N_{\rm BHNS,total}}$
- $f_{\rm b}(\theta_{\rm jet}) = 1 - \cos\theta_{\rm jet}$.
- $\mathcal{R}_{\rm BHNS}$ and $\mathcal{R}_{\rm DNS}$ are BHNS and DNS merger rates taking into account the SFR and metallicity evolution with read-shift as outlined in Bavera et al. (2020)

Results: GRB rate Predictions

Metallicity $[Z/Z_{\odot}]$	$f_{\text{jet,BHNS}}$	$f_{\text{jet,DNS}}$
0.5%	0.726	1.000
2%	0.803	1.000
10%	0.906	0.970
20%	0.471	1.000
30%	0.449	0.972
40%	0.408	1.000
50%	0.279	1.000
100%	0.429	1.000
150%	0.391	1.000

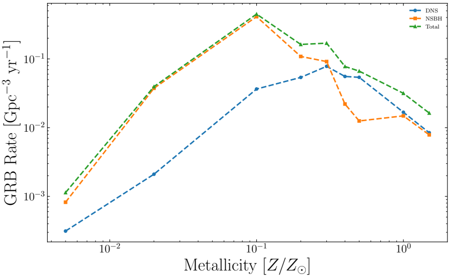

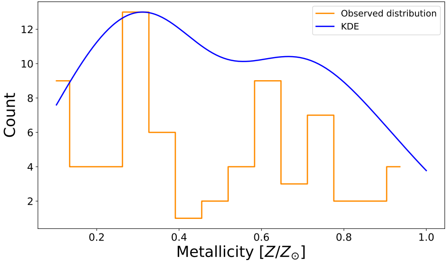

Torus Mass and GRB Energy from DNS Mergers

1. Torus Mass Estimation:

$$M_{\rm torus} = [c_1(1-q) + c_2]\,[c_3(1+q) - M_{tot}/M_{\rm max}]$$

- $q = M_2/M_1 \leq 1$ (mass ratio)
- $M_{\rm tot} = M_1 + M_2$ (total mass)
- $M_{\rm max}$ = maximum non-rotating NS mass (2.2 $M_\odot$)
- $c_1 = 2.974$, $c_2 = 0.11851$, $c_3 = 1.1193$

(Rezzolla et al. 2010) updated by Giacomazzo et al. (2013)

2. GRB Energy from the Torus Mass:

$$E_{\gamma,\rm iso} = \epsilon_{\rm jet} \cdot \epsilon_\gamma \cdot M_{\rm torus} \cdot c^2$$

Assumptions:

- $\epsilon_{\rm jet}$: Torus mass into jet energy efficiency (10%)
- ϵ_γ : jet energy into gamma rays efficiency (50%)

Why do this: In COSMIC $M_{\rm f} = M_1 + M_2$

Results: Torus mass

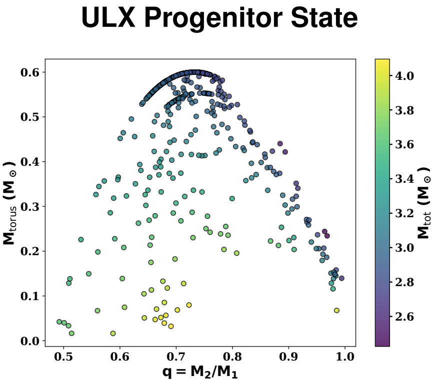

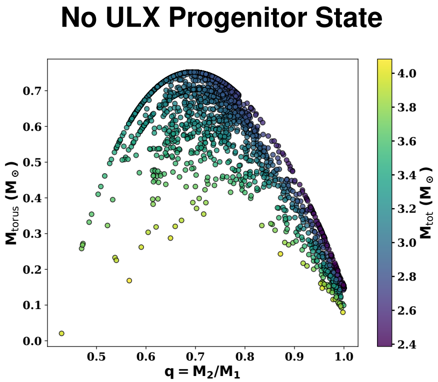

Results: Gamma-Ray Energy Distribution

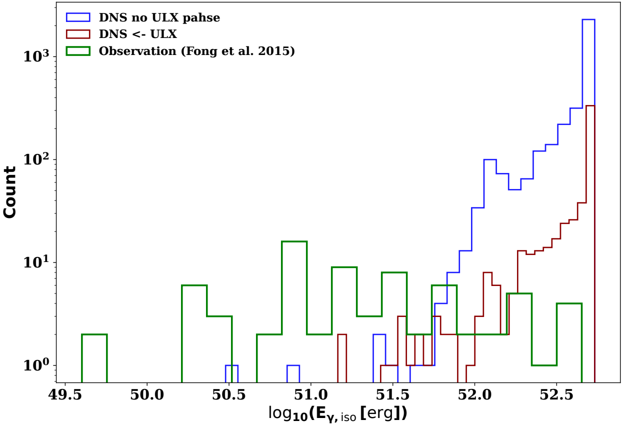

- Simulated populations show a similar energy range.

Summary and Limitations

Summary:

- 70-97 % of mDCO comes from the ULX phase, but only 10-20 % of mDNS comes from the ULX phase.
- SGRB metallicity distribution is comparable to the observed data.
- Gamma ray energy range is slightly higher than the observed range.

Limitations:

- Assumption 1: $f_{\mathrm{jet,DNS}} = \frac{N_{\mathrm{DNS->BH}}}{N_{\mathrm{DNS,total}}}$
  - Jet launching is expected when the remnant mass satisfies $M_{\mathrm{rem}} \gtrsim 1.2\, M_{\mathrm{TOV}} -> $ hypermassive NS, collapsing to a BH after a short delay.

Summary and Limitations

Limitations:

- Assumption 2: No condition on magnetic filed.
  - Initial magnetic filed $\sim 10^{12}$ G to produce poloidal filed of $\sim 10^{15}$ G (Rezzolla et al. 2010).
  - All our systems have $B < 10^{12}$ G

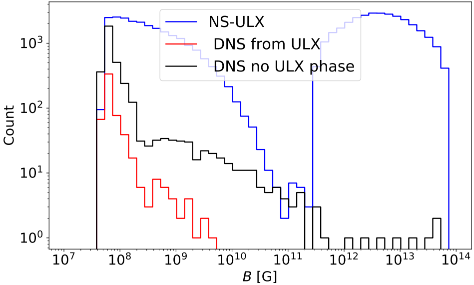

References

- Kroupa, P., Tout, C. A., & Gilmore, G. 1993, , 262, 545
- Vinokurov, A., Fabrika, S., & Atapin, K. 2013, *Astrophys. Bull.*, 68, 139
- Fabbiano, G., Kim, D.-W., & Trinchieri, G. 1989, , 347, 127
- Rezzolla, L., Baiotti, L., Giacomazzo, B., Link, D., & Font, J. A. 2010, *Class. Quantum Grav.*, 27, 114105
- Bavera, S. S., Fragos, T., Qin, Y., Zapartas, E., Neijssel, C. J., Mandel, I., Batta, A., Gaebel, S. M., Kimball, C., & Stevenson, S. 2020, , 635, A97
- Giacomazzo, B., Perna, R., Rezzolla, L., Troja, E., & Lazzati, D. 2013, , 762, L18
- Breivik, K., Rodriguez, C. L., Larson, S. L., & Kalogera, V. 2020, , 247, 24
- Fong, W., Berger, E., Margutti, R., & Zauderer, B. A. 2015, , 815, 102

Thank You!